

Development of Test Procedures to Evaluate Moisture Susceptibility of Asphalt Mixtures Used in the State of Kansas, Phase I: Surface Free Energy of Binders

Payal Verma
Masoud Darabi, Ph.D., P.E.

The University of Kansas



1 Report No. KS-24-06	2 Government Accession No.	3 Recipient Catalog No.	
4 Title and Subtitle Development of Test Procedures to Evaluate Moisture Susceptibility of Asphalt Mixtures Used in the State of Kansas, Phase I: Surface Free Energy of Binders		5 Report Date October 2024	
		6 Performing Organization Code	
7 Author(s) Payal Verma; Masoud Darabi, Ph.D., P.E.		8 Performing Organization Report No.	
9 Performing Organization Name and Address The University of Kansas Department of Civil, Environmental & Architectural Engineering 1530 West 15th St Lawrence, Kansas 66045-7609		10 Work Unit No. (TRAIS)	
		11 Contract or Grant No. C2126	
12 Sponsoring Agency Name and Address Kansas Department of Transportation Bureau of Research 2300 SW Van Buren Topeka, Kansas 66611-1195		13 Type of Report and Period Covered Final Report August 2018 – September 2022	
		14 Sponsoring Agency Code RE-0771-01	
15 Supplementary Notes For more information write to address in block 9.			
16 Abstract <p>The surface free energy of asphalt binders and aggregates is a critical material property related to the moisture sensitivity of asphalt mixtures. Surface free energies of these materials can be used to quantitatively determine the interfacial adhesive bond strength between two materials and the tendency of water to displace this bond based on fundamental principles of thermodynamics. Because the utilization of surface free energies to determine the moisture sensitivity of asphalt mixtures is already well established, efficient, and accurate methods to routinely measure the surface energies of asphalt binders and aggregates are needed to enhance material selection when designing moisture-resistant asphalt mixtures. Surface energies of these materials can also be combined with other material properties in conjunction with the principles of fracture mechanics to determine fatigue cracking and healing characteristics of asphalt mixtures.</p> <p>Therefore, the results from this study that calculates surface free energy components of different Asphalt binders can be used to select test methods and mathematical models based on fracture mechanics that relate material properties, including surface energy, to asphalt mixture performance. Surface energies of these materials can be used to calculate the energy ratio (ER) of asphalt binder-aggregate combinations to identify moisture resistance levels. A higher value of work of adhesion indicates that more work is required to break the adhesive bond between the asphalt binder and the aggregate, implying improved resistance to moisture damage. A lower magnitude of work of debonding indicates less energy potential for water to displace an asphalt binder from its interface with the aggregate and a higher resistance to moisture damage.</p>			
17 Key Words Binders, asphalt mixtures, moisture content, test procedures		18 Distribution Statement No restrictions. This document is available to the public through the National Technical Information Service www.ntis.gov .	
19 Security Classification (of this report) Unclassified	20 Security Classification (of this page) Unclassified	21 No. of pages 53	22 Price

Form DOT F 1700.7 (8-72)

This page intentionally left blank.

Development of Test Procedures to Evaluate Moisture Susceptibility of Asphalt Mixtures Used in the State of Kansas, Phase I: Surface Free Energy of Binders

Final Report

Prepared by

Payal Verma
Masoud Darabi, Ph.D., P.E.

The University of Kansas

A Report on Research Sponsored by

THE KANSAS DEPARTMENT OF TRANSPORTATION
TOPEKA, KANSAS

and

THE UNIVERSITY OF KANSAS
LAWRENCE, KANSAS

October 2024

© Copyright 2024, **Kansas Department of Transportation**

NOTICE

The authors and the state of Kansas do not endorse products or manufacturers. Trade and manufacturers names appear herein solely because they are considered essential to the object of this report.

This information is available in alternative accessible formats. To obtain an alternative format, contact the Office of Public Affairs, Kansas Department of Transportation, 700 SW Harrison, 2nd Floor – West Wing, Topeka, Kansas 66603-3745 or phone (785) 296-3585 (Voice) (TDD).

DISCLAIMER

The contents of this report reflect the views of the authors who are responsible for the facts and accuracy of the data presented herein. The contents do not necessarily reflect the views or the policies of the state of Kansas. This report does not constitute a standard, specification or regulation.

Abstract

The surface free energy of asphalt binders and aggregates is a critical material property related to the moisture sensitivity of asphalt mixtures. Surface free energies of these materials can be used to quantitatively determine the interfacial adhesive bond strength between two materials and the tendency of water to displace this bond based on fundamental principles of thermodynamics. Because the utilization of surface free energies to determine the moisture sensitivity of asphalt mixtures is already well established, efficient, and accurate methods to routinely measure the surface energies of asphalt binders and aggregates are needed to enhance material selection when designing moisture-resistant asphalt mixtures. Surface energies of these materials can also be combined with other material properties in conjunction with the principles of fracture mechanics to determine fatigue cracking and healing characteristics of asphalt mixtures.

Therefore, the results from this study that calculates surface free energy components of different asphalt binders can be used to select test methods and mathematical models based on fracture mechanics that relate material properties, including surface energy, to asphalt mixture performance. Surface energies of these materials can be used to calculate the energy ratio (ER) of asphalt binder-aggregate combinations to identify moisture resistance levels. A higher value of work of adhesion indicates that more work is required to break the adhesive bond between the asphalt binder and the aggregate, implying improved resistance to moisture damage. A lower magnitude of work of debonding indicates less energy potential for water to displace an asphalt binder from its interface with the aggregate and a higher resistance to moisture damage.

Acknowledgments

The authors would like to thank the Kansas Department of Transportation (KDOT) for providing the financial and logistical support for the research described in this report, and the University of Kansas for providing technical support. Thank you also to Mr. Kent Dye and Mr. David Woody of the University of Kansas for their assistance in installing KU asphalt lab equipment, and Htet Yatti Win for their assistance with data collection.

Table of Contents

Abstract	v
Acknowledgments	vi
Table of Contents	vii
List of Tables	ix
List of Figures	ix
Chapter 1: Introduction	1
1.1 Background	1
1.1.1 Surface Energy of Materials	1
1.1.2 Work of Adhesion between Two Materials	2
1.1.3 Work of Cohesion	2
1.1.4 Propensity of One Material to Displace Another from an Interface	3
1.2 Problem Statement	5
Chapter 2: Research Scope	7
2.1 General Methodology to Measure Surface Energy Components	7
2.1.1 Typical Range of Surface Energy Components of Asphalt Binders	7
2.1.2 Selection of Appropriate Probe Liquids	7
2.1.3 Importance of Advancing and Receding Contact Angles	12
2.2 Materials Used	14
2.3 Test Procedure	16
2.4 Calculations	21
Chapter 3: Results and Discussion	23

3.1 Surface Free Energy of Binders	23
3.1.1 Computing Surface Energies from Contact Angles.....	25
3.1.2 Computing Work of Adhesion and Energy Ratio of Asphalt Binder with Aggregates	32
3.1.3 Advantages and Limitations of the Wilhelmy Plate Device.....	34
3.2 Future Research.....	34
Chapter 4: Conclusions.....	35
References.....	36
Appendix A.....	38

List of Tables

Table 2.1:	Surface Free Energy Components of Probes (ergs/cm ²)	8
Table 2.2:	Advancing Contact Angle with Probe Liquids.....	9
Table 2.3:	Maximum and Minimum Advancing Contact Angle for Probe Liquids with Binder PG 64-28.....	11
Table 2.4:	Asphalt Binder Inventory	15
Table 2.5:	Various Apparatus Used in Study	16
Table 3.1:	Advancing Contact Angle Measures of Asphalt Binders with Probe Liquids	25
Table 3.2:	Surface Energy Components of Calculated Asphalt Binders.....	30
Table 3.3:	Surface Energy Components of Asphalt Binders Calculated at Texas A&M University	31
Table 3.4:	Surface Energy Components of Asphalt Binders Calculated at the University of Kansas.....	32

List of Figures

Figure 1.1: Adhesive Failure in a Material	4
Figure 1.2: Work of Debonding.....	5
Figure 2.1: Effect of Probe on Calculated Values	10
Figure 2.2: Advancing Contact Angles of Probe Liquids with Binder PG 64-28	12
Figure 2.3: Schematic Representation of Wilhelmy Plate Technique	17
Figure 2.4: Prepared Slides in the Slotted Slide Holder	18
Figure 2.5: Prepared Slide in the Beaker with Probe Liquid	19
Figure 2.6: Instrument and Software Setup in the Lab	20
Figure 2.7: Summary of Results from OneAttension Software	21
Figure 3.1: Surface Energy Components of Calculated Asphalt Binders.....	31

Chapter 1: Introduction

1.1 Background

Hot mix asphalt (HMA) is a composite material that primarily consists of mineral aggregates bound with an asphalt binder. Premature failure in HMA pavements is most often caused by moisture damage due to the loss of cohesion/adhesion and the tendency of water to displace the bond between aggregate and binder. Therefore, test methods and specification guidelines are essential to select compatible aggregate-binder (unmodified and modified) pairs that are resistant to moisture degradation. Quantification of adhesion between the asphalt binder and aggregate is possible if the surface free energies of both materials are known, and the fundamental principles of fracture mechanics can be used to model and predict the growth of fatigue cracks using a combination of surface free energy and other intrinsic material properties. However, the inability to measure the surface free energy components of asphalt binders and aggregates accurately and efficiently has hindered material selection, thereby preventing the improvement of asphalt mixtures. This research sought to determine and/or develop efficient test methods to routinely measure surface free energy components of asphalt binders. This report focuses on surface energy measurement to quantitatively determine the relationship between the surface free energy of asphalt binders and aggregates to asphalt mixture performance.

1.1.1 Surface Energy of Materials

Molecules within a material bulk are surrounded by other molecules, meaning they have a higher level of bond energy compared to molecules on a material's surface. Therefore, significant effort is required to extract molecules from the bulk and create a new area of surface molecules. This effort is referred to as the surface free energy of the material. The most common units of surface free energy are ergs/cm^2 or mJ/m^2 .

Although several theories explain the molecular origin of surface free energy of solids, the two-component theory and the acid-base theory are the most popular. The Good-van Oss-Chaudhury (GvOC) theory, or acid-base theory, is commonly applied to explain the surface energy components of various materials. According to this theory, a material's total surface free energy is comprised of three components based on the type of molecular forces on the surface: the nonpolar

component (i.e., the Lifshitz-van der Waals [LW] or dispersive component), the Lewis acid component, and the Lewis base component. The total surface free energy is obtained by combining these components as follows:

$$\gamma = \gamma^{LW} + \gamma^{\pm} = \gamma^{LW} + \sqrt{2 \gamma^+ \gamma^-}$$

Equation 1.1

Where:

γ = the total surface free energy of the material,

γ^{LW} = the LW or dispersive component,

γ^+ = the acid-base component,

γ^* = the Lewis acid component, and

γ^- = the Lewis base component (Howson et al., 2007).

1.1.2 Work of Adhesion between Two Materials

According to the acid-base theory, the work of adhesion, W^{AB} , between materials A and B can be expressed as a function of their respective surface free energy components as follows:

$$W^{AB} = 2 \gamma_A^{LW} \gamma_B^{LW} + 2 \gamma_A^+ \gamma_B^- + 2 \gamma_A^- \gamma_B^+$$

Equation 1.2

The phenomenological explanation for the work of adhesion is the amount of external work that is required to separate two materials at their interface in a vacuum (Figure 1.1). For an asphalt binder-aggregate system, Equation 1.2 is used to compute the work of adhesion when the surface free energy components of both materials are known (Little & Bhasin, 2007).

1.1.3 Work of Cohesion

The work of cohesion of a liquid is defined as the work required to separate a column of liquid with a unit cross-sectional area in two parts (Little & Bhasin, 2007). This definition can also pertain to solids. Using the definition of surface free energy, the total work of cohesion, W^{AA} , of material A can be derived as

$$W^{AA} = 2 \gamma^A$$

Equation 1.3

Where:

γ^A = the surface energy of the material.

The work of cohesion of asphalt binders is used in basic fracture-mechanics equations to determine energy required for microcrack growth within the asphalt binder phase or mastic phase of the asphalt mixture.

1.1.4 Propensity of One Material to Displace Another from an Interface

To quantify the propensity of one material to displace another, the interfacial energies of the materials must be known. An interface is a particular type of surface that forms a common boundary between two different materials. Figure 1.1 shows an idealized representation of an interface between materials A and B. The molecules of both materials at the interface are subjected to unequal forces compared to their respective bulk molecules, creating a misbalance of forces at the interface that results in interfacial energy (γ^{AB}) between the materials. The interfacial energy between two materials is defined as the work required to create a unit area of the interface by separating the two materials in a vacuum (Little & Bhasin, 2007). The relationship between the work of adhesion between two materials, the total surface energy of the two materials, and their interfacial energy is given by

$$W^{AB} = \gamma^A + \gamma^B - \gamma^{AB}$$

Equation 1.4

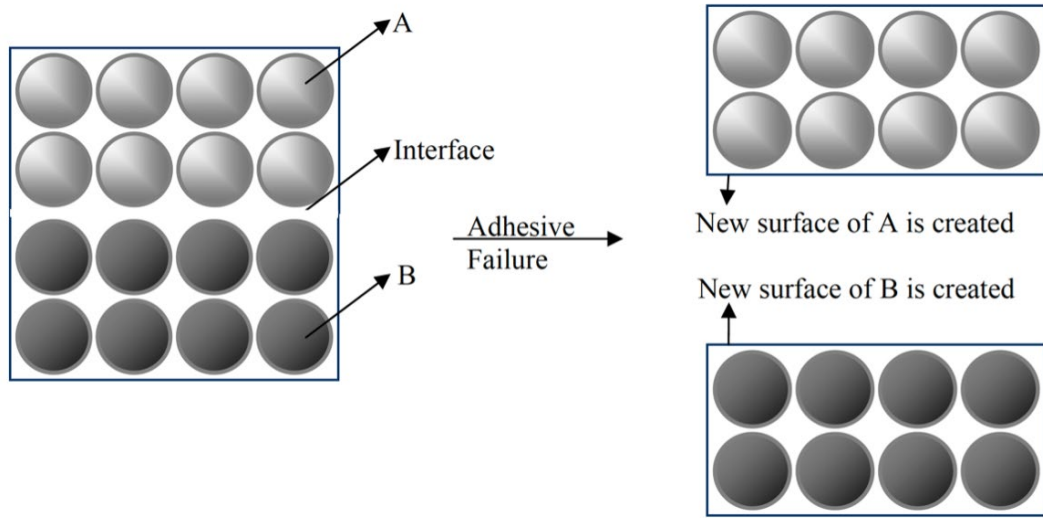


Figure 1.1: Adhesive Failure in a Material

Source: Little and Bhasin (2007)

Previous equations 1.3 and 1.4 have been combined to determine the interfacial energy between two materials when their individual surface energy components are known. In a three-phase system containing asphalt binder, aggregate, and water (represented by B, A, and W, respectively, in Figure 1.2), a process occurs in which water displaces the asphalt binder from the binder-aggregate interface. First, the interface of the aggregate with the binder is broken (AB), requiring external work $-\gamma^{AB}$, and then new interfaces between water and binder (BW) and between water and aggregate (AW) are created. The work to form these two new interfaces is $\gamma^{WB} + \gamma^{WA}$. Therefore, the total work for water to displace binder from the surface of the aggregate is $\gamma^{WB} + \gamma^{WA} - \gamma^{AB}$. If the displacement process is thermodynamically favorable, then it must demonstrate an overall decrease in free energy of the system. In other words, the total work done on the system during the displacement process must be less than zero. Results from this research confirmed this assertion for almost all asphalt binder-aggregate systems, suggesting that the displacement of asphalt binder by water is a thermodynamically favored phenomenon. In the context of adhesive failure of binder-aggregate bond, energy associated with binder displacement by water from the bitumen-aggregate interface, or debonding, is referred to as the work of debonding, expressed as

$$W^{ABW} = \gamma^{AW} + \gamma^{BW} - \gamma^{AB}$$

Equation 1.5

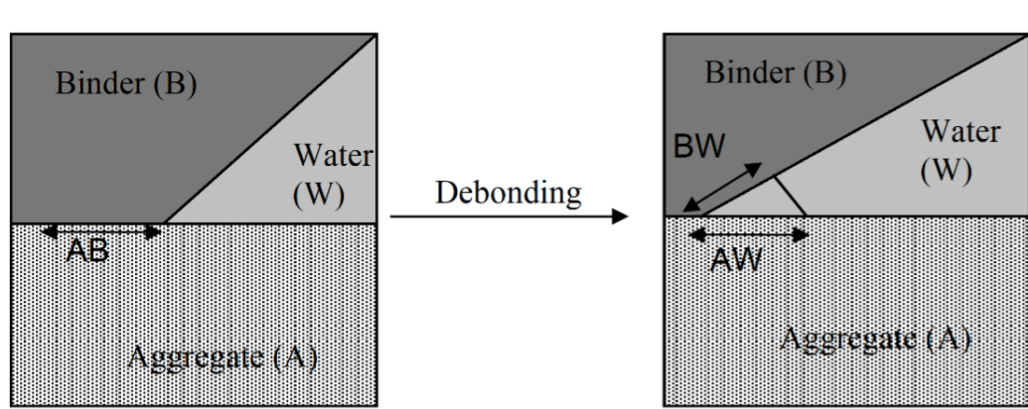


Figure 1.2: Work of Debonding

Source: Little and Bhasin (2007)

The magnitude of the work of debonding is a function of the surface energy components of the asphalt binder and aggregate. Accordingly, the potential for water to displace binder depends on the surface energy components of the binder and the aggregate (Little & Bhasin, 2007).

1.2 Problem Statement

Moisture damage is the primary distress that causes premature failure in HMA pavements. The loss of cohesion/adhesion and the tendency of water to displace the bond between aggregate and binder are the major mechanisms that lead to moisture damage. Therefore, test methods and specification guidelines must be developed and enhanced to select aggregate-binder (unmodified and modified) pairs that are compatible and resistant to moisture degradation.

The current state of practice at the Kansas Department of Transportation (KDOT) and many other agencies is to conduct mechanical tests on moisture-conditioned and dry specimens to evaluate moisture susceptibility of asphalt mixtures. However, these simple tests may be unreliable due to the following deficiencies:

- Poor correlation with field performance,
- Substantial variability in test results and lack of repeatability,

- Inability to address specific failure mechanisms and underlying root causes,
- Extended testing time, and
- Required repetition of tests when slight modifications are made (e.g., addition of modifiers).

These deficiencies have led KDOT researchers to evaluate the efficacy of applying more fundamental lab tests and characterization methods to determine moisture susceptibility of asphalt mixtures. Therefore, current research must identify an efficient test method to select asphalt concrete constituents that result in moisture damage-resistant asphalt mixtures.

Chapter 2: Research Scope

2.1 General Methodology to Measure Surface Energy Components

The primary objective of this analysis was to characterize the surface energy components for a suite of asphalt binders. Based on the literature review, the following candidate test methods were identified for determining the surface energy components of asphalt binders: the Wilhelmy plate method (WP), the sessile drop method, atomic force microscopy (AFM), and inverse gas chromatography (IGC). This research utilized the Wilhelmy plate method, meaning the surface energy components of thirty types of asphalt binders were measured using three types of probe liquids whose surface free energy components are already known.

2.1.1 Typical Range of Surface Energy Components of Asphalt Binders

The total surface energy of asphalt binder typically has a range of 15–45 ergs/cm². The LW component is the most significant contributor to the total surface energy, and based on results from the Wilhelmy plate test, the LW varies significantly depending on the binder type. Most asphalt binders have exceedingly small magnitudes of the acid or base component, typically 0–3 ergs/cm², because most asphalt binders are weak acids or bases. These small magnitudes can be scaled when multiplied with larger magnitudes of the acid–base components of the aggregate while computing the work of adhesion (Little & Bhasin, 2007).

Because the direct measurement of surface energy components of a solid is rarely feasible, the more efficient way to determine the surface energy components of materials such as asphalt binders is to experimentally measure a manifestation of the surface energy of these materials in physical interactions using probe liquids or vapors.

2.1.2 Selection of Appropriate Probe Liquids

The work of adhesion between a solid and at least three probe liquids is measured using a suitable experimental technique, while the work of adhesion with various liquids is combined using an equation to determine the three surface energy components of the solid. Any liquid may be used as a probe if it satisfies the following criteria:

- The three surface energy components of the probe liquid must be known based on the acid-base theory at the test temperature.
- The probe liquid must be chemically homogenous and pure.
- The probe liquid must not interact chemically with the investigated solid surface. For example, the liquid must not dissolve or chemically react with the solid.
- If the probe liquid is used to measure contact angles over a solid surface, then the surface energy of the probe liquid must be greater than the anticipated surface energy of the solid.

Table 2.1 lists five liquids that satisfy the criteria and were used with asphalt binders in this research. However, only three probe liquids are required to determine the three unknown surface energy components of any material by measuring their interfacial work of adhesion and solving for unknown components in Equation 1.2. Contact angles for at least three replicate samples were measured with each probe liquid for each asphalt binder at ambient temperature, approximately 68 °F (20 °C).

Table 2.1: Surface Free Energy Components of Probes (ergs/cm²)

Probe Liquid/ Vapor	γ^{LW}	γ^+	γ^-	γ^{Total}
Water	21.8	25.5	25.5	72.8
Glycerol	34	3.92	57.4	64
Formamide	39	2.28	39.6	58
Ethylene Glycol	29	1.92	47	48
Methylene Iodide	50.8	0	0	50.8
Hexane	18.4	0	0	18.4
Methyl propyl ketone (MPK)	21.7	0	19.6	21.7

Table 2.2 summarizes the contact angles of the asphalt binders with various probes measured using the Wilhelmy plate method, including standard deviations.

Table 2.2: Advancing Contact Angle with Probe Liquids

		Replicate 1	Replicate 2	Replicate 3	Average of 3	Standard Deviation
PG64- 28	Water	96.58	96.29	96.11	96.33	0.24
	Glycerol	86.80	86.51	87.06	86.79	0.28
	Formamide	85.63	83.67	83.56	84.28	1.17
	Ethylene glycol	72.03	72.64	72.71	72.46	0.37
PG70- 20	Water	103.30	102.86	102.04	102.73	0.64
	Glycerol	90.70	91.04	90.86	90.87	0.17
	Formamide	85.08	83.79	83.76	84.21	0.76
	Ethylene glycol	74.62	74.75	74.43	74.60	0.16
PG70- 22	Water	99.72	98.27	97.26	98.41	1.24
	Glycerol	85.36		85.63	85.49	0.19
	Formamide		84.01	83.68	83.85	0.23
	Ethylene glycol	71.39	71.55	71.09	71.35	0.23

If the surface energy components of the selected probe liquids are within 10 percent of each other, the calculated surface free energy components of the solid (asphalt binder or aggregate) will become unduly sensitive to the measured physical property, especially when only a limited set of liquids is used to estimate the surface energy components of the solid. For example, when y is measured via probes with characteristic x , and the calculated parameter of interest is the slope of y vs. x , if two probes with similar values of x are selected, then the difference between the measured value of y will be small. This theoretically minimal difference is compounded by experimental error leading to variability in calculated value of slope.

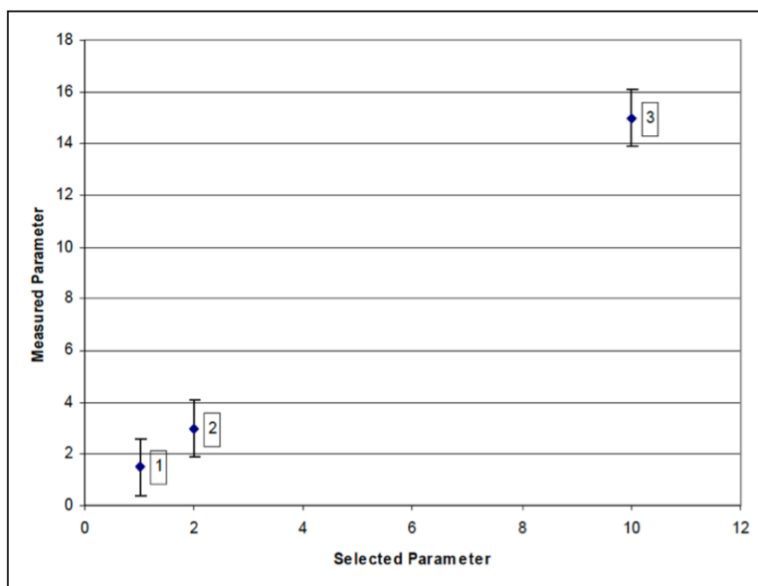


Figure 2.1: Effect of Probe on Calculated Values

Source: Little and Bhasin (2007)

More specifically, if probes 1 and 2 with hypothetical values of x as 1 and 2, respectively, are used to measure physical property y , the difference in the slope (which is the parameter of interest computed using x and y) will increase. However, if a third probe is used with an x value that differs significantly from the values of the other two probes and the measured parameter y is like the other y , then the variability in the calculated slope decreases (Figure 2.1). Mathematically, this scenario can be represented as

$$\text{Slope} = \frac{y_2 - y_1}{x_2 - x_1}$$

Equation 2.1

If $x_2 - x_1$ is small, its reciprocal would be large, implying that the error in measuring y_2 and y_1 is increased by a greater degree. The above illustration Figure 2.1 presents a simplified scenario of a poor choice of liquids, especially when a limited set of liquids is used to determine surface properties. Liquids must be selected so that the calculated surface energies represent reasonable estimates of the true value with minimal error, such as a mathematical measure that is the condition

number of the selected set of liquids. The smaller the condition number, the less sensitive the calculated results are to the experimental error.

Table 2.3 lists the maximum and minimum advancing contact angle of the four probe liquids (Table 2.2) with binder PG 64-28, and Figure 2.2 plots the four probe liquids with their surface free energy in x-axis and minimum and maximum advancing contact angle with binder PG 64-28 in y axis.

Table 2.3: Maximum and Minimum Advancing Contact Angle for Probe Liquids with Binder PG 64-28

	γ^{Total} (ergs/cm ²)	Max θ (degrees)	Min θ (degrees)
Water	72.8	96.58	96.11
Glycerol	64	87.06	86.51
Formamide	58	85.63	83.56
Ethylene glycol	48	72.71	72.03

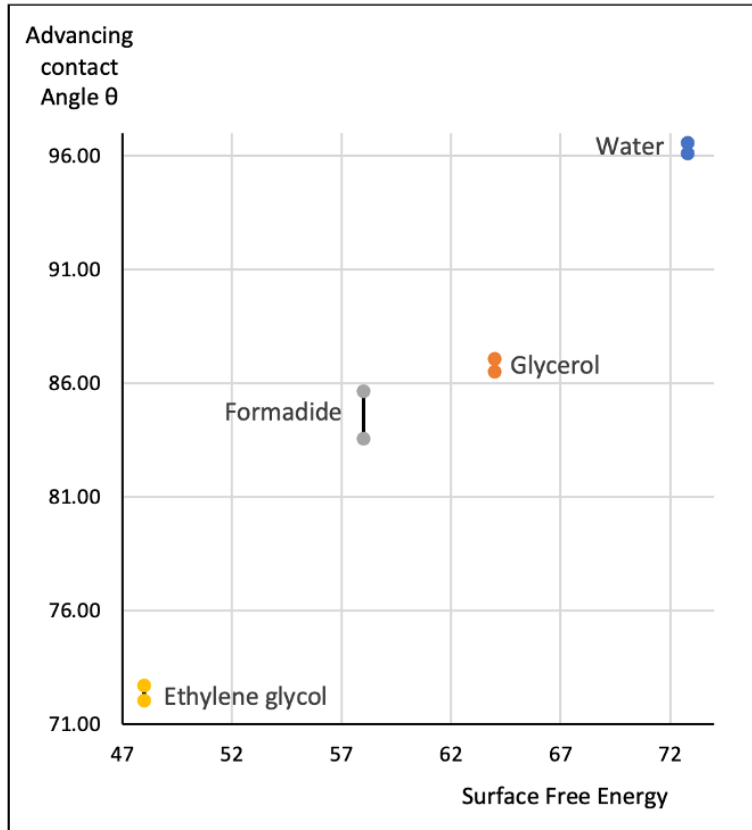


Figure 2.2: Advancing Contact Angles of Probe Liquids with Binder PG 64-28

Probes used in further analysis were water, glycerol, and ethylene glycol. Although the dispersion of the measured parameters y (contact angles) for these probes is small, the probes had distinct values of the selected parameter x (total surface energy parameter). Therefore, variability in the calculated slope was low.

2.1.3 Importance of Advancing and Receding Contact Angles

Differences in the advancing and receding contact angle are referred to as contact angle hysteresis. Under ideal conditions, hysteresis should be zero (i.e., the advancing and receding contact angles should be identical for a given solid surface). Contact angles measured via the Wilhelmy plate method almost always demonstrate hysteresis. Kwok et al. (1997) and Kwok et al. (1998) found that physical roughness of the solid surface and chemical heterogeneity are two plausible causes for hysteresis. In the Wilhelmy plate method, samples of the asphalt binder are prepared by coating a thin glass slide with molten binder. The sample is prepared at elevated

temperatures with the binder in a liquid state. As the sample cools, the fundamental intermolecular forces responsible for surface energy ensure a minimal surface area. Therefore, samples prepared using this method are not likely to demonstrate roughness at the micro scale. Because the chemical heterogeneity of asphalt binders is well established, the hysteresis of contact angles with asphalt binders can reasonably be attributed to chemical heterogeneity rather than physical roughness.

The use of advancing contact angles to calculate the surface free energy components and work of adhesion is supported by the literature (Harkins & Cheng, 1921; Della Volpe & Siboni, 2000). The calculation of surface free energy components of solids from receding contact angles is, in principle, as correct as the resulting calculation from advancing contact angle because both of them correspond to metastable states. For clarity, *apparent* surface free energy components could refer to values calculated from receding angles to emphasize that the contact angle in the calculation is not measured at equilibrium. Although the surface science community typically uses sessile static contact angles, which they consider to be measured at equilibrium, or base surface free energy calculations on advancing contact angles, no accepted method exists to measure the true equilibrium value of a contact angle by distinguishing it from an infinite number of other metastable values. Thus, all calculated values of solid surface free energy available in the literature are *apparent* unless they stem from (nearly) ideal surfaces, which is rare.

For heterogeneous surfaces, valuable results from Johnson and Dettre (1964) and Johnson et al. (1977) prove that both advancing and receding contact angles are representative, with advancing contact angles correlating with the low-energy portion of the surface and receding contact angles correlating with the high-energy one. If the two *apparent* contact angles provide a more in-depth description of the surface than the Young contact angle, then this reasoning could logically be extended to the calculation of surface free energy. However, previous works (Della Volpe, 2000; Jacobasch et al., 1995) indicate that the receding contact angles can also be used as an index of surface energy. Receding contact angles are measured when the binder sample is withdrawn from the probe liquid or during the de-wetting process of the asphalt binder with the probe liquid. The receding contact angle is associated with the fracture properties of the material instead of the advancing contact angle, which is measured in the wetting process and is associated with the healing characteristics of the material (Lytton, n. d.).

2.2 Materials Used

Table 2.4 lists the various KDOT asphalt binders used in this research. Base asphalt binders were modified by the manufacturer to produce 12 modified asphalt binders. These modifications were achieved by introducing additives such as styrene-butadiene-styrene (SBS), liquid anti-stripping agent (0.5 % LOF), and polymer modified bitumen (PMB) to the base asphalt binder. The exact nature, amount, and process of modification varied, but the details were not disclosed to the authors. In the table, the asphalt binders are labeled by the Performance Grade (PG) grade, followed by the type of modifier. For example, binder 64-22 B indicates PG 64-22 binder and a base (B) or unmodified binder. A binder with the label 76-28 SBS indicates grade PG 76-28 with modification via SBS. Table 2.5 lists the various apparatus used in this research.

Table 2.4: Asphalt Binder Inventory

	Performance Grade	Lab Number	Estimated Amount (g)
1	58-28	18-0209	788
2	64-22	18-0210	685
3	64-28	18-0414	1327
4	64-28	18-0224	852
5	52-34	18-0412	702
6	58-28	18-0413	650
7	64-34	18-0415	578
8	70-28	18-0416	690
9	58-34	18-0225	866
10	64-22	18-0264	701
11	58-28	18-0316	779
12	64-22	18-0299	640
13	64-22	18-0315	800
14	70-28 (0.5% LOF)	18-0009	802
15	76-28 (modified)	18-0274	771
16	58-34	18-0039	649
17	64-28 (0.5% LOF)	18-0010	782
18	64-28 (0.5% LOF)	18-0011	764
19	76-28 (SBS)	18-0045	706
20	64-28 (SBS)	18-0048	590
21	70-22 (SBS)	18-0042	656
22	64-34 (P/PMB)	18-0040	767
23	70-34 (P)	18-0047	774
24	76-28 (modified)	18-0136	746
25	64-28	18-0184	691
26	70-28 (0.5% LOF)	18-0008	787
27	58-28	18-0133	750
28	70-28 (modified)	18-0135	815
29	58-28	18-0211	905
30	64-28	18-0537	663
31	64-22	18-0134	735

Table 2.5: Various Apparatus Used in Study

	Apparatus	Description and Use
1	Wilhelmy Plate Device	This device contains a microbalance with a motor-controlled stage that can be raised or lowered at desired speed to immerse a slide with asphalt binder in the probe liquid in advancing mode and to withdraw the slide from the probe liquid in receding mode.
2	Oven	This apparatus is capable of heating up to 300 °F (150 °C) as is required to heat asphalt binders for sample preparation.
3	Heating Plate	Temperature control is required to maintain the temperature of the asphalt binder during the sample preparation process.
4	Microscope Glass Plates	Plates measuring 24 mm x 60 mm (about 0.94 x 2.36 in.) (no. 1.5) serve as substrates for the asphalt binder and a vernier caliper to measure the dimensions of the slide.
5	Slotted Slide Holder	This apparatus is required to hold the finished asphalt binder slides.
6	OneAttension Software	This data acquisition and analysis software collects the data and determines the contact angle.

2.3 Test Procedure

A Wilhelmy plate device was used to determine the three surface energy components of asphalt binders. This method was used with the mathematical analysis manual to determine surface energy components from contact angle measurements and the computerized spreadsheets developed to carry out this analysis.

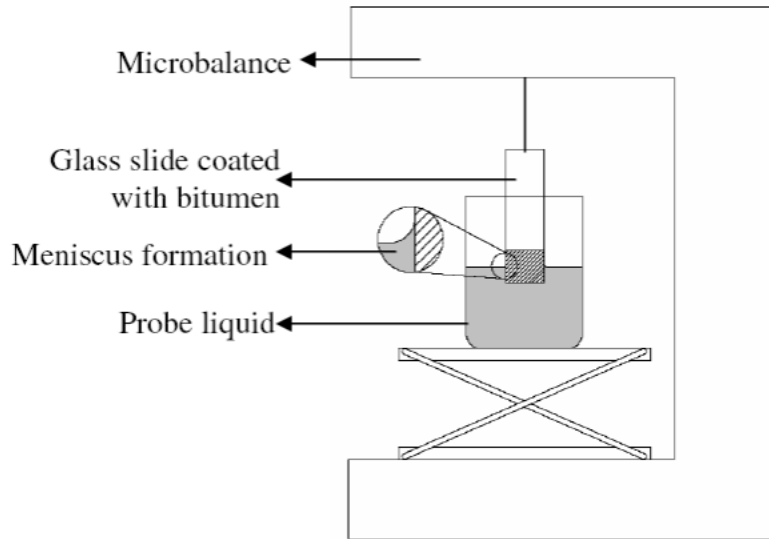


Figure 2.3: Schematic Representation of Wilhelmy Plate Technique

Source: Little and Bhasin (2007)

The first step in the research was to obtain the representative sample material based on AASHTO Standards T40 Sampling of Bituminous Materials (2012). Approximately 1.75 ounces (50 g) of each asphalt binder were stored in small metallic containers for this test. The container with asphalt binder was heated in an oven for approximately 1 hour until it reached the mixing temperature, and then it was placed over a heating plate to maintain the mixing temperature. The end of the glass slide intended for coating was passed through the blue flame of a propane torch to remove any moisture. This slide was dipped into the molten bitumen to about 15 mm (about 0.59 in.) deep, and the excess binder could drain from the plate until a very thin (0.18–0.35 mm) and uniform layer remained on it. The uniform thickness of the asphalt binder was confirmed on both sides of the slide throughout its width and for at least 10 mm (about 0.39 in.) from the edge to be immersed in the probe liquid. A thin coating reduces variability of the results. The prepared slides were carefully placed in the slotted slide holder for 24 hours (Figure 2.4).

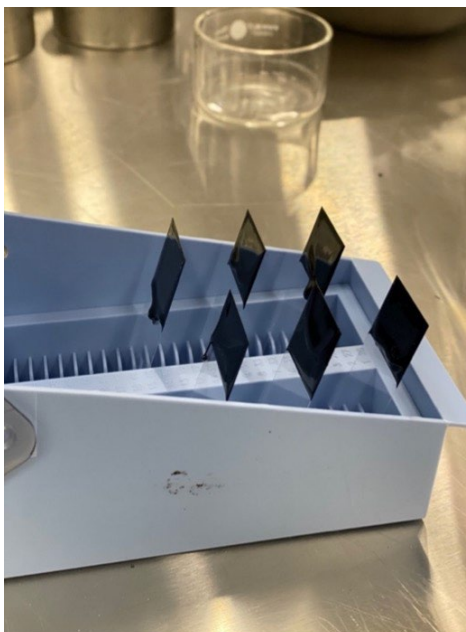


Figure 2.4: Prepared Slides in the Slotted Slide Holder

On the following day, once the microbalance was calibrated in accordance with manufacturer specifications, the following experiment was performed on each replicate of the asphalt binders:

1. The width and thickness of each asphalt binder coated slide was measured to an accuracy of 0.01 mm to calculate its perimeter. The measurements were made just beyond 8 mm (about 0.31 in.) from the edge of the slide to avoid contaminating the portion of coating to be immersed in the probe liquid.
2. Each asphalt binder coated glass slide was suspended from the microbalance using a crocodile clip to ensure that the slide was horizontal with respect to the base of the balance. A clean glass beaker was filled with probe liquid to a depth of at least 10 mm (about 0.39 in.) and placed on the balance stage. The stage was raised manually to bring the top of the probe liquid to the bottom edge of the slide (Figure 2.5).

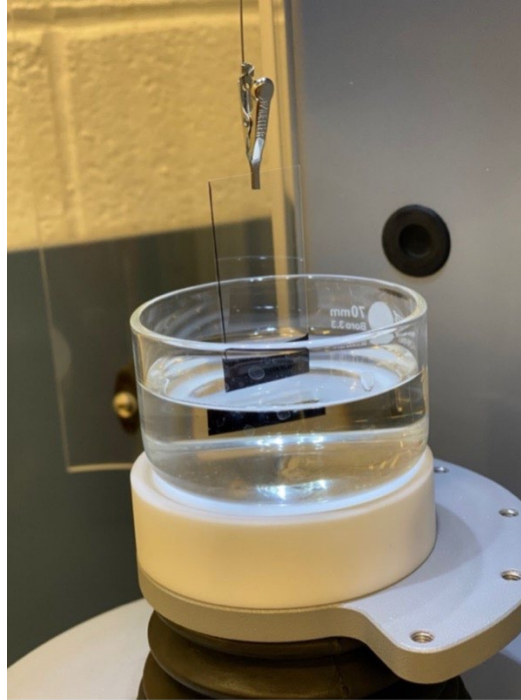


Figure 2.5: Prepared Slide in the Beaker with Probe Liquid

3. During the test, the stage was raised or lowered at the desired rate via a stepper motor controlled by the OneAttension software (Figure 2.6). A rate of 40 microns per second was recommended to achieve quasi-static equilibrium conditions for contact angle measurement. The depth to which the sample was immersed in the probe liquid was set to 8 mm (about 0.31 in.). Depths up to 15 mm (about 0.59 in.) were acceptable if the thickness of the asphalt coating on the slide was uniform. The weight of the slide measured by the microbalance was recorded continuously by the software accompanying the device during the advancing (stage raised to dip the slide) and receding (stage lowered to retract the slide from the liquid) processes.

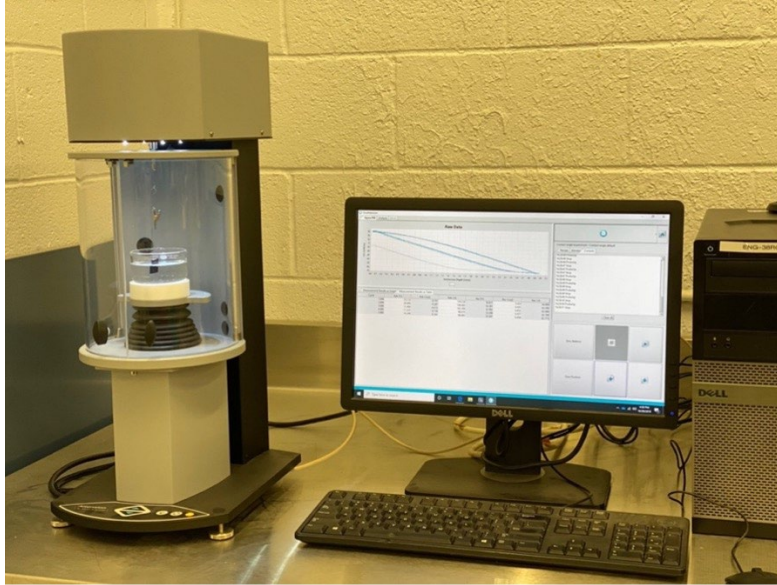
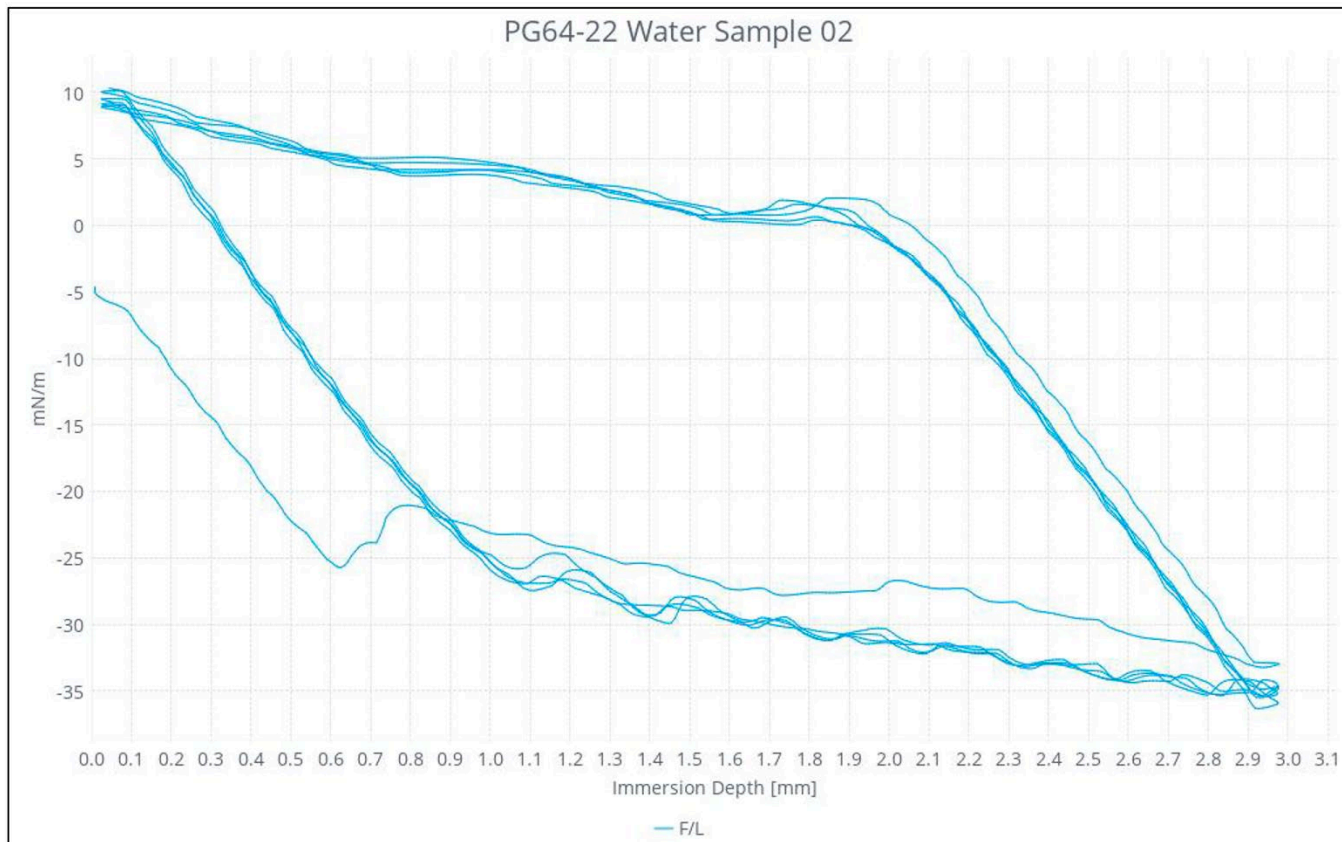


Figure 2.6: Instrument and Software Setup in the Lab

4. Water, ethylene glycol, and glycerol were the three probe liquids recommended for this test. All reagents had to be high-purity grade (>99%), and contact angles had to be measured for at least three replicates with each probe liquid for each asphalt binder.
5. The probe liquid in the beaker was disposed after testing with three asphalt binder slides, and a fresh sample of the probe liquid was used for each binder type. All probe liquids were stored in airtight containers, and liquids were not recommended for use after prolonged exposure to air in open-mouthed beakers.
6. Tests were completed 24–36 hours from the time the slides were prepared.

After all five increments were completed in the force tensiometer, the software produced a force per meter versus immersion depth graph and the advancing and receding contact angles in each cycle along with the linear force (Figure 2.7).



Detailed results

Cycle	Adv F/L	Adv Cos()	Adv CA	Rec F/L	Rec Cos()	Rec CA
1.000	-12.159	-0.168	99.681	8.924	0.123	82.910
2.000	-23.292	-0.322	108.793	8.556	0.118	83.203
3.000	-24.076	-0.333	109.451	8.894	0.123	82.934
4.000	-23.181	-0.321	108.701	9.495	0.131	82.454
5.000	-21.871	-0.303	107.608	9.867	0.136	82.156

Figure 2.7: Summary of Results from OneAttension Software

2.4 Calculations

The difference between the weight of a plate measured in air and a plate partially submerged in a probe liquid (ΔF) is expressed in terms of buoyancy of the liquid, liquid surface

energy, contact angle, and geometry of the plate. The contact angle between the liquid and surface of the plate is calculated from this equilibrium as

$$\cos\theta = \frac{\Delta F + V_{im}(\rho_L - \rho_{air}g)}{P_t \gamma_L^{Tot}}$$

Equation 2.2

Where:

P_t = the perimeter of the bitumen coated plate,

γ_L^{Tot} = the total surface energy of the liquid,

θ = the dynamic contact angle between the bitumen and the liquid,

V_{im} = the volume immersed in the liquid,

ρ_L = the density of the liquid,

ρ_{air} = the air density, and

g = the local acceleration due to gravitation.

The accompanying software requires the density of the liquid, total surface tension of the liquid, dimensions of the sample, and local acceleration due to gravity as inputs to compute the contact angle using force measurements from the microbalance. However, because buoyancy correction based on slide dimensions and liquid density can introduce unwanted variability into the resulting contact angles, the software performed a regression analysis of the buoyancy line and extrapolated the force to zero depth. The advancing and receding contact angles were based on the representative area of the line for regression analysis using the equation. If the force measurements were not smooth (i.e., sawtooth-like force measurements due to slip-stick behavior between the probe liquid and the asphalt binder), they were reported with the advancing and receding contact angles. The typical standard deviation of the measured contact angle for each pair of liquid and asphalt binder based on measurements with three replicate slides was less than 2°. The contact angle of each replicate and probe liquid was used with the surface energy analysis workbook that conducts the required analysis to determine the three surface energy components of the asphalt binder and the standard deviations of these components (Howson et al., 2007).

Chapter 3: Results and Discussion

Moisture damage in asphalt mixtures can occur within the asphalt binder phase (cohesive fracture) or at the aggregate-asphalt interface (adhesive fracture or failure). Whether or not a cohesive or adhesive failure occurs depends on the physio-chemical nature and the relative thickness of the mastic. Previous studies on this subject have developed tests and empirical parameters that quantify moisture sensitivity of whole asphalt mixtures, but the primary objective of this research was to develop a framework to evaluate moisture damage by considering fundamental material properties and mechanisms that influence durability of the adhesive interface between aggregate and asphalt and the cohesive strength and durability of the mastic.

The material property related to the moisture sensitivity of asphalt mixtures is the surface free energy of the asphalt binder and the aggregate. Surface free energies of these materials can be used to quantitatively determine the interfacial adhesive bond strength between these two materials and the tendency of water to displace this bond based on fundamental principles of thermodynamics. The importance of surface free energies of asphalt binder and aggregate for determining the moisture sensitivity of asphalt mixtures is well established. Therefore, efficient and accurate methods to routinely measure the surface energies of asphalt binders and aggregates can enhance material selection for designing moisture-resistant asphalt mixtures. Surface energies of these materials can also be combined with other material properties and used with the principles of fracture mechanics to determine fatigue cracking and healing characteristics of asphalt mixtures. This project evaluated asphalt surface energy to calculate moisture susceptibility of various asphalt-aggregate combinations.

3.1 Surface Free Energy of Binders

KDOT provided 30 binders for this research, and asphalt binder tests were conducted using a force tensiometer and the Wilhelmy plate technique at the asphalt lab at the University of Kansas (KU). In this test, the contact angle between the microscope glass slide plate coated with asphalt and standard probe liquids with known surface energies were measured in both advancing and receding modes. Three liquid probes of water, ethylene glycol, and glycerol were selected as

standard probe liquids of known surface free energy components. The surface energy of the asphalt was determined based on these measurements.

This research initially sought to calculate the contact angle of asphalt binders with different probe liquids. Two replicates of each asphalt binder were tested with three liquid probes. Once the test was conducted on all the binder replicates, the surface free energy components of these binders were calculated using

$$\gamma = \gamma^{LW} + \gamma^{\pm} = \gamma^{LW} + \sqrt{2\gamma^+\gamma^-}$$

Equation 3.1

Table 3.1 shows the contact angle measures for 30 asphalt binders with three probe liquids obtained from the experiments.

Table 3.1: Advancing Contact Angle Measures of Asphalt Binders with Probe Liquids

S. No.	Asphalt Binder		Advancing Contact Angle (degrees)		
	Performance Grade		Water	Ethylene Glycol	Glycerol
1	PG 58-28	18-0209	88.64	121.72	111.29
2	PG 64-22	18-0210	77.03	110.63	99.52
3	PG 64-28	18-0414	42.30	108.60	84.56
4	PG 64-28	18-0224	73.01	105.96	100.89
5	PG 52-34	18-0412	24.64	83.37	45.92
6	PG 58-28	18-0413	55.60	119.92	79.23
7	PG 64-34	18-0415	27.55	95.91	31.02
8	PG 70-28	18-0416	49.73	110.97	87.62
9	PG 58-34	18-0225	46.54	93.96	99.43
10	PG 64-22	18-0264	44.65	75.80	44.53
11	PG 58-28	18-0316	98.81	101.57	101.51
12	PG 64-22	18-0299	108.00	105.12	98.72
13	PG 64-22	18-0413	97.66	99.21	97.73
14	PG 70-28 (0.5% LOF)	18-0009	109.66	141.32	119.50
15	PG 76-28 (modified)	18-0274	43.92	116.94	84.35
16	PG 58-34	18-0039	135.42	124.67	139.00
17	PG 64-28 (0.5% LOF)	18-0010	61.09	108.03	95.25
18	PG 64-28 (0.5% LOF)	18-0011	55.07	108.28	75.68
19	PG 76-28 (SBS)	18-0045	111.14	99.20	105.14
20	PG 64-28 (SBS)	18-0048	105.28	122.75	116.12
21	PG 70-22 (SBS)	18-0042	107.58	98.94	94.22
23	PG 70-34 (P)	18-0047	107.40	111.24	108.48
24	PG 76-28 (modified)	18-0136	64.30	108.35	90.40
25	PG 64-28	18-0184	61.28	137.04	97.28
26	PG 70-28 (0.5% LOF)	18-0008	45.06	114.38	72.35
27	PG 58-28	18-0133	118.08	155.43	114.86
28	PG 70-28 (modified?)	18-0135	54.01	110.66	80.56
29	PG 58-28	18-0211	115.31	108.39	112.87
30	PG 64-28	18-0537	43.77	115.04	76.79
31	PG 64-22	18-0134	100.01	105.01	102.64

3.1.1 Computing Surface Energies from Contact Angles

The surface energy component of a solid surface is determined by measuring its contact angles with various probe liquids. This section presents two methods to determine surface energy components and standard deviations of a solid using three liquids. The first method utilizes

singular value decomposition according to Della Volpe and Siboni (2000) and Della Volpe and Siboni (1997); the second method uses weighted least squares.

Based on the Young-Dupre equation (neglecting the spreading pressure), work of adhesion is expressed as follows:

$$w = W_{adhesion}/2 = 0.5\gamma(1 + \cos\theta)$$

Equation 3.2

Where:

γ = the total surface free energy of the probe liquid, and

θ = the contact angle of the probe liquid on the surface of the solid.

The equation for a set of probe liquids is

$$0.5\gamma_{li}(1 + \cos\theta_i) = \sqrt{\gamma_{li}^{LW}\gamma_s^{LW}} + \sqrt{\gamma_{li}^+\gamma_s^-} + \sqrt{\gamma_{li}^-\gamma_s^+}$$

Equation 3.3

Where:

γ = the total surface free energy,

γ^{LW} = the LW component of surface free energy,

γ^- = the Lewis acid component of surface free energy,

γ^+ = the Lewis base component of surface free energy,

subscript li = the i^{th} liquid (where i = the number of probe liquids used), and

subscript s = the solid surface.

If the actual number of liquids used is 3, then the system of linear equations generated from the Equation 3.3 is

$$\mathbf{A x = B}$$

Equation 3.4

Where:

$$\mathbf{A} = \begin{bmatrix} \sqrt{\gamma_{l1}^{LW}} & \sqrt{\gamma_{l1}^+} & \sqrt{\gamma_{l1}^-} \\ \sqrt{\gamma_{l2}^{LW}} & \sqrt{\gamma_{l2}^+} & \sqrt{\gamma_{l2}^-} \\ \sqrt{\gamma_{l3}^{LW}} & \sqrt{\gamma_{l3}^+} & \sqrt{\gamma_{l3}^-} \end{bmatrix}, \mathbf{x} = \begin{bmatrix} \sqrt{\gamma_s^{LW}} \\ \sqrt{\gamma_s^-} \\ \sqrt{\gamma_s^+} \end{bmatrix}, \mathbf{B} = 0.5 \begin{bmatrix} \gamma_{li}(1 + \cos\theta_1) \\ \gamma_{li}(1 + \cos\theta_2) \\ \gamma_{li}(1 + \cos\theta_3) \end{bmatrix}$$

Equation 3.5

Since only three probe liquids were used in this research, the number of equations was equal to the number of unknowns, and the equations could be solved. In this case, matrix A is a square matrix and vector X with the square roots of unknown components of the solid can be solved if A is nonsingular as follows:

$$\mathbf{x} = \mathbf{A}^{-1}\mathbf{B}$$

Equation 3.6

However, because this study used nonlinear terms involving decision variables x , an optimization problem was utilized to determine the optimal combination of x . A focus of this research was the identification of x such that $AX = B$, which could then minimize deviation D or error E given by $AX - B$. Various techniques in the literature address this error minimization problem using the error term E , meaning any of the following three quantities could be minimized:

1. Mean absolute deviation (MAD): As the most common error measurement tool, it calculates the average of the absolute value of a series of errors. By using the absolute values, this tool prevents the positive and negative errors from canceling each other out. A lower value of MAD corresponds to higher accuracy.

$$MAD = \frac{\sum_{i=1}^n |A_i - F_i|}{n}$$

Equation 3.7

2. Mean absolute percentage error (MAPE): This technique measures the mean or average of the absolute percentage errors of a series of measurements. Error is defined as the difference between the actual and the observed value. A smaller MAPE means improved accuracy of the method.

$$MAPE = \frac{100}{n} \sum_{i=1}^n \frac{|A_i - F_i|}{A_i}$$

Equation 3.8

3. Mean square error (MSE): MSE measures the average of the squares of the errors, thereby amplifying a smaller magnitude of errors.

$$MSE = \frac{\sum_{i=1}^n (A_i - F_i)^2}{n}$$

Equation 3.9

Study results showed that Mean Absolute Deviation (MAD) yielded the least number of errors across all the computational experiments. Python code for the three models is provided in Appendix A. The three matrices were utilized as objective functions in the nonlinear optimization problem. Results of the unconstrained model indicated that the values of the decision variables (i.e., γ^{LW} , γ^+ , and γ^-) were outside the acceptable ranges for twelve out of thirty instances. Most asphalt binders have very small magnitudes of the acid or base component, typically 0–3 ergs/cm², which necessitates the incorporation of a constraint of $\gamma^+ < 3$ ergs/cm² and $\gamma^- < 3$ ergs/cm². Moreover, the total surface energy of an asphalt binder is usually 15–45 ergs/cm², and the LW component is the most significant contributor to the total surface energy based on the relationship given by

$$\gamma = \gamma^{LW} + \gamma^{\pm} = \gamma^{LW} + \sqrt{2\gamma^+\gamma^-}$$

Equation 3.10

Thus, a constraint of the form $\gamma^{LW} + \sqrt{2\gamma^+\gamma^-}$ with a range of 15–45 ergs/cm² is justified.

Two methods can be used to incorporate $\gamma^{LW} + \sqrt{2\gamma^+\gamma^-}$ falling in a range of 15–45 ergs/cm² constraints into the optimization problem. First, the constraint can be treated as hard constraints, thereby requiring the parameter values to lie in the specific ranges. Results of this experimental analysis showed that this hard constraint strategy leads to superior performances in most instances. Notably, this study executed three separate models for the constrained versions of the optimization problem, utilizing MAD, MAPE, and MSE as the objective function, and the optimal solution among the models was extracted. Table 3.2 shows the surface free energy components of asphalt binders calculated according to this method. Results showed that the constrained optimization model produced acceptable values for decision variables in 10 instances. In some cases, however, the value of γ^{LW} was not in the range of 15–45 ergs/cm², and occasionally the constraint $\gamma^+ < 3$ ergs/cm² and $\gamma^- < 3$ ergs/cm² did not yield acceptable solutions. Therefore, this study employed higher values of the threshold and found that using the constraint $\gamma^+ < 8$ ergs/cm² and $\gamma^- < 8$ ergs/cm² yielded values of parameters in acceptable range.

Table 3.2: Surface Energy Components of Calculated Asphalt Binders

S. No.	Asphalt Binder		Surface Free Energy Components (ergs/cm ²)			
	Grade		γ^{LW}	γ^+	γ^-	γ^{total}
1	PG 58-28	18-0209	19.785	2.993	1.406	22.686
2	PG 64-22	18-0210	32.585	2.993	1.742	35.815
3	PG 64-28	18-0414	22.074	2.804	2.703	25.968
4	PG 64-28	18-0224	14.935	2.993	0.000	14.935
5	PG 52-34	18-0412	1.382	83.654	15.499	52.306
6	PG 58-28	18-0413	60.599	2.993	2.046	64.099
7	PG 64-34	18-0415	92.216	2.993	0.000	92.216
8	PG 70-28	18-0416	102.674	2.993	0.000	102.674
9	PG 58-34	18-0225	16.015	2.993	0.000	16.015
10	PG 64-22	18-0264	97.054	2.993	0.000	97.054
11	PG 58-28	18-0316	59.042	2.993	0.000	59.042
12	PG 64-22	18-0299	17.713	1.016	0.007	17.829
13	PG 64-22	18-0413	0.000	14.968	5.840	13.223
14	PG 70-28 (0.5% LOF)	18-0009	0.283	2.993	0.000	0.283
15	PG 76-28 (modified)	18-0274	0.000	110.375	3.587	28.139
16	PG 58-34	18-0039	3.319	0.151	0.000	3.319
17	PG 64-28 (0.5% LOF)	18-0010	30.379	2.993	0.735	32.477
18	PG 64-28 (0.5% LOF)	18-0011	39.150	2.993	0.000	39.150
19	PG 76-28 (SBS)	18-0045	2.314	3.413	1.883	5.899
20	PG 64-28 (SBS)	18-0048	9.000	0.640	0.640	9.905
21	PG 70-22 (SBS)	18-0042	24.958	2.992	1.734	28.180
23	PG 70-34 (P)	18-0047	20.458	2.993	1.098	23.021
24	PG 76-28 (modified?)	18-0136	114.724	2.993	0.111	115.538
25	PG 64-28	18-0184	101.911	2.993	0.000	101.911
26	PG 70-28 (0.5% LOF)	18-0008	45.316	2.993	0.017	45.632
27	PG 58-28	18-0133	0.000	3.427	3.860	5.144
28	PG 70-28 (modified?)	18-0135	51.557	2.993	1.127	54.155
29	PG 58-28	18-0211	3.826	2.993	0.332	5.235
30	PG 64-28	18-0537	56.929	2.993	1.146	59.548
31	PG 64-22	18-0134	17.384	7.396	0.384	19.768

Figure 3.1 shows the distribution of γ^{total} . As shown in the figure, half of the values lie in the accepted range of 15–45 ergs/cm², but various outliers may be due to the difficulty in solving the optimizing problem, experimental design, and calibration and human error.

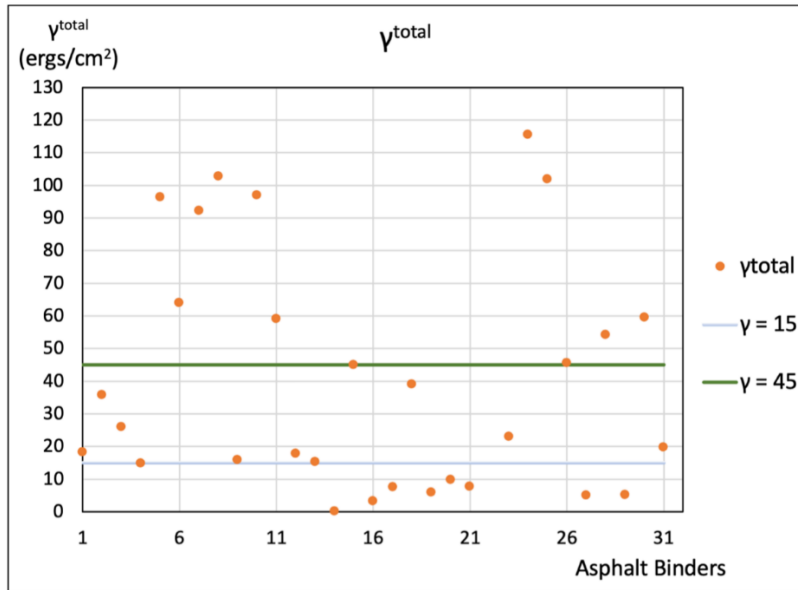


Figure 3.1: Surface Energy Components of Calculated Asphalt Binders

Six of the asphalt samples were also tested at Texas A&M University; Table 3.3 shows their computed results. The results of the same six binders tested at KU are tabulated in Table 3.4.

Table 3.3: Surface Energy Components of Asphalt Binders Calculated at Texas A&M University

Asphalt Binder			Surface Free Energy Components (ergs/cm ²)			
	S. No.	Grade	γ^{LW}	γ^+	γ^-	γ^{total}
Neat	1	PG58-28	14.049	5.9748	4.2214	24.093
	5	PG52-34	0.019	33.292	20.015	51.647
	13	PG64-22	0	87.725	13.21	68.083
Modified	15	PG76-28 (modified)	1.47E-20	39.444	10.448	40.602
	17	PG64-28 (0.5%LOF)	12.77	2.7067	18.667	26.986
	21	PG70-22 (SBS)	15.542	10.786	5.0477	30.299

Table 3.4: Surface Energy Components of Asphalt Binders Calculated at the University of Kansas

Asphalt Binder			Surface Free Energy Components (ergs/cm ²)			
S. No.	Grade		γ^{LW}	γ^+	γ^-	γ^{total}
1	PG 58-28	18-0209	19.785	2.992	1.405	22.686
5	PG 52-34	18-0412	1.382	83.654	15.499	52.306
13	PG 64-22	18-0413	0	14.968	5.840	13.223
15	PG 76-28 (modified)	18-0274	1.72E-33	110.375	3.586	28.139
17	PG 64-28 (0.5% LOF)	18-0010	30.379	2.992	0.734	32.477
21	PG 70-22 (SBS)	18-0042	24.958	2.991	1.734	28.18

As shown in the tables, the results for the six binders tested at KU were similar to the results from Texas A&M. Any dissimilarities could be due to differences in the environmental temperature for testing and varied sample preparation techniques. Also, tests at Texas A&M utilized five probe liquids, but reported results of three probe liquids considered for calculations, while KU tests used three probe liquids, which limited the calculations to the available data.

3.1.2 Computing Work of Adhesion and Energy Ratio of Asphalt Binder with Aggregates

The surface energy components of several unmodified and modified asphalt binders were determined and cataloged using Whilhelmy plate device test procedure. The typical range of values for the surface energy components, work of cohesion and adhesion, and energy parameters with different aggregates were determined to guide future measurements. In this research, an energy-based parameter, or energy ratio (ER), was used to calculate moisture susceptibility using the following equation for known surface energy measurements:

$$ER = \left| \frac{W^{AB} - W^{BB}}{W^{ABW}} \right|$$

Equation 3.11

This parameter can be used as a screening tool to select binders and aggregates with the maximum resistance to moisture damage.

According to the acid-base theory, the work of cohesion, W^{BB} of the asphalt binder, the work of adhesion, W^{AB} , between materials A and B, and the work of debonding when water displaces asphalt binder from its interface with the aggregate can be expressed as a function of their respective surface free energy components as follows:

$$W^{BB} = 2 \gamma^B$$

$$W^{AB} = 2 \gamma_A^{LW} \gamma_B^{LW} + 2 \gamma_A^+ \gamma_B^- + 2 \gamma_A^- \gamma_B^+$$

$$W^{ABW} = \gamma^{AW} + \gamma^{BW} - \gamma^{AB}$$

Equation 3.12

An example of the use of ER computed using the surface energy components of asphalt binders and aggregates is an aggregate limestone with surface energy components γ^{LW} 58.89 ergs/cm², γ^+ 18.82 ergs/cm², and γ^- 561.11 ergs/cm² and asphalt binder PG 70-28 with surface energy components γ^{LW} 26.05 ergs/cm², γ^+ 0.0003543 ergs/cm², and γ^- 3 ergs/cm². Therefore, the work of adhesion between these two binders and aggregate is 160.55 ergs/cm², the cohesive bond energy of the asphalt binder is 52.23 ergs/cm², and the magnitude of work of debonding is 180 ergs/cm². The computed parameter, ER, for this combination of asphalt binder PG 70-28 and limestone is then 0.601. A higher value of W^{AB} indicates that more work is required to break the adhesive bond between the asphalt binder and the aggregate, implying improved resistance to moisture damage. A lower magnitude of W^{ABW} indicates less energy potential for water to displace an asphalt binder from its interface with the aggregate and a higher resistance to moisture damage.

This study also developed a system to evaluate the influence of fundamental material properties, mixture modification, and mixture design on moisture susceptibility. In this system, an energy-based parameter (ER) can be calculated using the surface energy measurements and then used as a screening tool to select binders and aggregates with the maximum resistance to moisture damage.

3.1.3 Advantages and Limitations of the Wilhelmy Plate Device

The Wilhelmy plate device is available commercially and requires minimal financial investment for laboratory preparations. The device usually comes with a user-friendly control and analysis software to conduct the test and analyze results. The test procedure is quite simple and requires minimal training. Asphalt binder samples for this test are prepared by immersing a thin glass slide in a molten binder and then allowing the coated slides to cool, which limits the potential to alter the chemical state of the binder during sample preparation. Another advantage of this test method is that the measured contact angle is an average over an infinite number of boundaries that are created as the sample is very slowly immersed into the probe liquid to a depth of approximately 5 mm (about 0.20 in.). The advancing and receding contact angles are automatically measured during each test.

In most cases the Wilhelmy plate device does not come equipped with an environmental chamber for stringent temperature control. Therefore, ambient temperature must be in reasonable proximity to the test temperature. This limitation in temperature setting also prevents contact angles from being measured at different test temperatures. However, the simplicity of the Wilhelmy plate method and its relatively low capital outlay make it an ideal choice for use as a routine test method to measure surface energy components of asphalt binders.

3.2 Future Research

The framework and tentative protocols developed in this project can be used to select appropriate asphalt binders for any aggregates to design mixtures with the maximum resistance to moisture damage. Compared to traditional methods that only test whole mixtures, this framework is based on a bottom-up approach to quantify moisture sensitivity of asphalt mixtures. As such, the results of this project can help reduce asphalt pavement failures due to moisture damage, leading to longer pavement life with less maintenance and construction costs. Also, identifying combinations of asphalt and aggregates that bond well together will expand the options of acceptable alternative sources of aggregates and asphalt binders for any project.

Chapter 4: Conclusions

The surface free energy of an asphalt binder and aggregate is essential for determining the moisture susceptibility of asphalt mixtures. This project proposed an efficient method to routinely measure the surface energies of asphalt binders and aggregates to help design asphalt mixtures that are increasingly resistant to moisture damage. Surface energies of these materials can be used to calculate the energy-based parameter (ER) of asphalt binder-aggregate combinations to identify moisture resistance levels. Due to variability in the results, at least four probe liquids should be used in the future to enhance calculation accuracy. In addition, future tests should be conducted in a controlled environment that limits significant temperature change. Results from this analysis could be used to select test methods and mathematical models that relate surface energy to the performance of asphalt mixtures.

References

- AASHTO T 40. (2012). *Standard method of test for sampling bituminous materials*. American Association of State Highway and Transportation Officials.
- Della Volpe, C., & Siboni, S. (1997). Some reflections on acid-base solid surface free energy theories. *Journal of Colloid and Interface Science*, 195(1), 121-136. <https://doi.org/10.1006/jcis.1997.5124>
- Della Volpe, C., & Siboni, S. (2000). Acid-base surface free energies of solids and the definition of scales in the Good-van Oss-Chaudhury theory. *Journal of Adhesion Science and Technology*, 14(2), 235-272. <https://doi.org/10.1163/156856100742546>
- Harkins, W. D., & Cheng, Y. C. (1921). The orientation of molecules in surfaces. VI. Cohesion, adhesion, tensile strength, tensile energy, negative surface energy, interfacial tension, and molecular attraction. *Journal of the American Chemical Society*, 43(1), 35-53. <https://doi.org/10.1021/ja01434a006>
- Howson, J. E., Masad, E. A., Bhasin, A., Branco, V. C., Arambula, E., Lytton, R. L., & Little, D. (2007). *System for the evaluation of moisture damage using fundamental material properties* (Report No. FHWA/TX-07/0-4524-1). Texas Transportation Institute. <http://tti.tamu.edu/documents/0-4524-1.pdf>
- Jacobasch, H. J., Grundke, K., Schneider, S., & Simon, F. (1995). Surface characterization of polymers by physico-chemical measurements. *Journal of Adhesion*, 48, 57-73. <https://doi.org/10.1080/00218469508028154>
- Johnson, R. E., & Dettre, R. H. (1964). Contact angle hysteresis. III. Study of an idealized heterogeneous surface. *Journal of Physical Chemistry*, 68(7), 1744-1750. <https://doi.org/10.1021/j100789a012>
- Johnson, R. E., Dettre, R. H., & Brandreth, D. A. (1977). Dynamic contact angles and contact angle hysteresis. *Journal of Colloid and Interface Science*, 62(2), 205-212. [https://doi.org/10.1016/0021-9797\(77\)90114-X](https://doi.org/10.1016/0021-9797(77)90114-X)

- Kwok, D. Y., Gietzelt, T., Grundke, K., Jacobasch, H. J., & Neumann, A. W. (1997). Contact angle measurements and contact angle interpretation: 1. Contact angle measurements by axisymmetric drop shape analysis and a goniometer sessile drop technique. *Langmuir*, *13*(10), 2880-2894. <https://doi.org/10.1021/la9608021>
- Kwok, D. Y., Leung, A., Lam, C. N. C., Li, A., Wu, R., & Neumann, A. W. (1998). Low-rate dynamic contact angles on poly (methyl methacrylate) and the determination of solid surface tensions. *Journal of Colloid and Interface Science*, *206*(1), 44-51. <https://doi.org/10.1006/jcis.1998.5610>
- Little, D. N., & Bhasin, A. (2007). Using surface energy measurements to select materials for asphalt pavement (NCHRP Web-Only Document 104). Transportation Research Board. <https://nap.nationalacademies.org/catalog/22001>
- Lytton R. L. (2006). Adhesive Fracture in Asphalt Concrete Mixtures. In *Asphalt Technology Handbook* (Youtcheff J., ed.), Marcel Dekker.

Appendix A

```
# -*- coding: utf-8 -*-
"""
Created on Sun Oct 16 20:07:33 2022
@author: Payal Verma
Solve for Ax = B for 31 different instances
"""
filename = 'b_matrix_values.csv'
f = open(filename)
lines = f.readlines()
ctr = 0
df = {}
for line in lines:
    if ctr != 0:
        lst = line.split(',')
        elems = [float(e) for e in lst]
        ky = int(elems[0])
        df[ky] = (elems[1],elems[2],elems[3])
    ctr += 1

# Define the list of results
# R = []
import numpy as np

# https://docs.scipy.org/doc/scipy/reference/generated/scipy.optimize.least\_squares.html
# "Solve a nonlinear least-squares problem with bounds on the variables."

import scipy.optimize as optimize

A = [[4.669,5.050,5.050],[5.385,1.386,6.856],[5.831,1.980,7.576]]
```

```
#Define your loss function
```

```
def f_MSE(x):
```

```
    #y = np.dot(A, x) - b
```

```
    yhat = np.dot(A,x)
```

```
    d = b - yhat
```

```
    return np.mean(d**2)
```

```
def f_MAD(x):
```

```
    #y = np.dot(A, x) - b
```

```
    yhat = np.dot(A,x)
```

```
    d = b - yhat
```

```
    return np.mean(abs(d))
```

```
def f_MAPE(x):
```

```
    actual = b
```

```
    pred = np.dot(A,x)
```

```
    mape = np.mean(np.abs((actual - pred) / actual)) * 100
```

```
    return mape
```

```
finalres = []
```

```
finalres.append(['id','startSol','obj','x','y','z','x+sqrt(2yz)'])
```

```
bnds = ((0, None), (0, None), (0, None))
```

```
startSols = [[0, 0, 0],[3, 0.8, 0.8],[6, 1.73, 1.73]]
```

```
objs = [f_MSE,f_MAD,f_MAPE]
```

```
strObjs = ['f_MSE','f_MAD','f_MAPE']
```

```
###TNC - Truncated Newton Method; L-BFHS-B - Bounded BFGS, Nelder Mead, SLSQP - Sequential Least  
Square Quadratic Program
```

```
from math import sqrt
```

```
for k in df.keys():
```

```

for s in startSols:
    itr = 0
    for f in objs:
        out = []
        out.append(k)
        out.append(s)
        out.append(strObjs[itr])
        itr += 1
        b = [df[k][0],df[k][1],df[k][2]]
        print(f)
        res = optimize.minimize(f, s, method='SLSQP', bounds=bnds, options={'disp': False})
        v = np.square(res.x)
        x = v[0]
        y = v[1]
        z = v[2]
        calc = x + sqrt(2*y*z)
        out.append(x)
        out.append(y)
        out.append(z)
        out.append(calc)
    finalres.append(out)

```

```

import csv
with open("results_out_full.csv", "w") as f:
    writer = csv.writer(f)
    writer.writerows(finalres)

```

